

**BENDING BEHAVIOUR OF A HYBRID FIBER
REINFORCED CONCRETE BEAMS**

**A Thesis Submitted to
the Graduate School
İzmir Institute of Technology
In Partial Fulfillment of the Requirements for the Degree of**

MASTER OF SCIENCE

In Civil Engineering

**by
Sarra ALOUI**

December 2020

İZMİR

ACKNOWLEDGEMENTS

I would like to thank the following people who have helped me undertake this research:

My supervisor Dr. Selçuk Saatci for his enthusiasm for the project, for his support, encouragement and patience.

The civil engineering department, IZMIR INSTITUTE OF TECHNOLOGY, for input throughout this MSc program.

My friends who have supported me and had to put up with my stresses and moans for the past three years of study.

And my biggest thanks to my family: my father Belgacem , my mother Ghazela, my sisters Asma and Chaima for all the support you have shown me through this research, the culmination of five years of distance learning.

ABSTRACT

BENDING BEHAVIOUR OF HYBRID FIBER REINFORCED CONCRETE BEAMS

Fiber reinforced concrete is widely used in various applications in concrete members. In this study, effect of fiber hybridization, using different types of fibers in concrete mix, on the bending behavior of concrete beams was investigated. For this purpose, eight beam specimens, 2500x500x50 mm in dimension, were cast in pairs with four different steel fiber content. One of the two specimens with the same steel fiber content had additional Polyvinyl Alcohol (PVA) fibers. The specimens were first tested under three-point bending. After these tests, failed specimens, which had a single crack at the midspan, were broken into two halves and the half with no visible damage was tested again under four-point loading to obtain the behavior for a constant moment region. The ultimate strength and the load-displacement behavior was investigated for each specimen. It was seen that fiber hybridization obtained by addition of PVA had an adverse effect for three-point bending tests. Specimens with additional PVA fibers had a lower ultimate load and deflection capacity compared to specimens with only steel fibers. However, fiber hybridization had a positive effect for some specimens under four-point bending test. It was concluded that hybridization of steel and PVA fibers had a positive effect on the bending behavior for loading conditions that result in a uniform moment distribution. However, for cases where a single crack dominates the behavior, such as a three-point bending case, hybrid fibers were not as effective or even had an adverse effect.

ÖZET

HİBRİT LİF KATKILI BETON KİRİŞLERİN EĞİLME DAVRANIŞI

Lif katkılı beton, çeşitli beton uygulamalarında yaygın olarak kullanılmaktadır. Bu çalışmada beton karışımında farklı tip liflerin kullanılmasıyla elde edilen lif hibritleşmesinin beton kirişlerin eğilme davranışı üzerine olan etkileri incelenmiştir. Bu amaçla 2500x500x50 mm boyutlarındaki sekiz kiriş çiftler halinde dört farklı çelik lif içeriğiyle dökülmüştür. Aynı çelik lif içeriğine sahip iki numuneden birine polivinil alkol (PVA) lifler eklenmiştir. Numuneler önce üç noktalı eğilme deneyine tabi tutulmuştur. Bu deneylerin sonrasında açıklık ortasından tek bir çatlakla göçen numuneleriki parçaya ayrılmış ve gözle görünür bir hasarı olmayan yarı parça, sabit moment bölgesi durumunda davranışı görmek amacıyla, tekrar dört noktalı eğilme deneyine tabi tutulmuştur. Her bir numune için taşıma gücü ve yük-yer değiştirme davranışı incelenmiştir. PVA lif eklenmesiyle elde edilen lif hibritleşmesinin üç noktalı eğilme deneylerinde olumsuz etki yaptığı görülmüştür. PVA lif eklenmiş numuneler sadece çelik lif içeren numunelere göre daha düşük taşıma gücü ve yer değiştirme kapasitesi göstermişlerdir. Ancak aynı numuneler dört noktalı eğilme deneylerine tabi tutulduklarında lif hibritleşmesi olumlu etkide bulunmuştur. Çelik ve PVA liflerin hibritleştirilmesinin yayılı moment dağılımı oluşturan yükleme durumlarında eğilme davranışında olumlu etkiye sahip olduğu sonucuna varılmıştır. Ancak üç noktalı eğilme durumunda olduğu gibi tek bir çatlağın davranışı belirlediği durumlarda hibrit liflerin etkili olmadığı, hatta olumsuz etkiye sahip olduğu görülmüştür.

TABLE OF CONTENTS

LIST OF FIGURES.....	vii
LIST OF TABLES	x
CHAPTER 1.INTRODUCTION	1
1. 1Objective.....	2
1. 2Thesis Organization.....	3
CHAPTER 2.LITERATURE REVIEW.....	4
2. 1Introduction	4
2. 2Types Of Fiber Reinforcement	4
2. 3Properties Of The Used Fibers:	5
2.3. 1 The Steel Fiber:	5
2.3. 2 Properties Of The Steel Fiber Reinforcement:.....	8
2.3. 3 Polyvinyl Alcohol Fibers (PVA):.....	11
2.3. 4 Effects Of Fibers On The Flexural Behavior Of Concrete Beams:.....	11
CHAPTER 3.EXPERIMENTAL WORK.....	15
3.1.Materials And Mix Proportions:	15
3.2.Specimen Preparation:.....	18
3.3.Testing Procedure.....	20
3.3.1.Three-point Bending Tests	20
3.3.2.Four-point Bending Tests	24
3.3.3.The Compression Tests:	25
CHAPTER 4.TEST RESULTS AND DISCUSSION	27
4.1.Three-point Bending Tests	27
4.1.1.SA1 And SA1+PVA	27
4.1.2.SA2 And SA2+PVA	29

4.1.3.SA3 And SA3+PVA	32
4.1.4.SA4 And SA4+PVA	34
4.1.5.Discussion Of Results For Three-point Bending Tests.....	37
4.2.Four-point Bending Tests	39
4.2.1.SA1a And SA1a+PVA.....	39
4.2.2.SA2a And SA2a+PVA.....	40
4.2.3.SA3a And SA3a+PVA.....	42
4.2.4.SA4a And SA4a+PVA.....	43
4.2.5.Discussion Of Results For Four-point Bending Tests	45
4.3.The Compression Tests Results :.....	48
CONCLUSION.....	52
REFERENCES	54

LIST OF FIGURES

<u>Figure</u>	<u>Page</u>
Figure 1. Typical load-deflection behavior of fiber reinforced concrete beams (aci 54, 1999).....	2
Figure 2. Steel fiber (kaur, 2017).....	5
Figure 3. Glass fiber (kaur, 2017).....	5
Figure 4. Synthetic fiber (kaur, 2017).....	5
Figure 5. Natural fiber (kaur, 2017).....	5
Figure 6 .Types of fiber reinforcement (kaur, 2017).....	6
Figure 7. Types of hooked ended steel reinforcement (“dramix,” n.d.).....	7
Figure 8. 3d hooked ended steel fiber(“dramix,” n.d.).....	8
Figure 9. 4d hooked ended steel fiber (“dramix,” n.d.).....	8
Figure 10. 5d hooked ended steel fiber(“dramix,” n.d.).....	8
Figure 11. Influence of the volume fraction of fibers on the compressive stress-strain (aci 544, 1999).....	9
Figure 12. Influence of the aspect ratio of fibers on the stress-strain curve.....	9
Figure 13. Stress-strain curves for steel fiber reinforced mortars in tension (aci 544, 1999).....	10
Figure 14. Characteristics of the load-deflection curve. (aci 544, 1999).....	11
Figure 15. Effect of beam depth on the flexural strength of the steel fiber.....	12
Figure 16. Flexural toughness ratio of the composites with different pva fiber.....	13
Figure 17. Load vs. Mid-span deflection for composites with different pva contents (zhang et al. 2019)......	13
Figure 18. The used steel fiber.....	16
Figure 19. The used pva fiber.	17
Figure 20. Rotation drum mixer.....	19
Figure 21. Formworks.....	19
Figure 22. Bending test mechanism.....	20
Figure 23. Loading point at the midspan.	21

<u>Figure</u>	<u>Page</u>
Figure 24. Test setup for three point bending	21
Figure 25. Linear resistive position transducer.	22
Figure 26. The disposition of linear resistive position transducers.	22
Figure 27. The disposition of the linear resistive position transducer after deflection. ..	22
Figure 28. The distribution of the beads for the three point bending test.	23
Figure 29. Placement of beads for three-point bending test.	23
Figure 30. Four-point bending tests, test setup.	24
Figure 31. Four-point bending tests.	24
Figure 32. Beads for the four-point bending test.	25
Figure 33. Placement of beads for four-point bending tests.	25
Figure 34. The cylinders ready to be tested.	26
Figure 35. The digital compression machine.	26
Figure 36. Load-midspan deflection response for sa1 and sa1+pva	27
Figure 37. Final view of sa1 after testing	28
Figure 38. Final view of sa1+pva after testing.	28
Figure 39. Section photo of sa1	28
Figure 40. Section photo of sa1+pva.....	29
Figure 41. Load-midspan deflection response for sa2 and sa2+pva.	30
Figure 42. Final view of sa2 after testing	30
Figure 43. Final view of sa2+pva after testing	31
Figure 44. Section photo of sa2	31
Figure 45. Section photo of sa2+pva.....	31
Figure 46. Load-midspan deflection response for sa3 and sa3+pva	32
Figure 47. Final view of sa3 after testing.	33
Figure 48. Final view of sa3+pva after testing	33
Figure 49. Section photo of sa3	33
Figure 50. Section photo of sa3+pva.....	34
Figure 51. Load-midspan deflection response for sa4 and sa4+pva.	35
Figure 52. Final view of sa4 after testing.	35
Figure 53. Final view of sa4+pva after testing.	35

<u>Figure</u>	<u>Page</u>
Figure 54. Section photo of sa4	36
Figure 55. Section photo of sa4+pva.....	36
Figure 56. Maximum loads for three-point bending tests.	37
Figure 57. Maximum moments for three-point bending tests.	38
Figure 58. Load-midspan deflection response for sa1a and sa1a+pva.....	39
Figure 59. Final view of sa1a after testing.	39
Figure 60. Final view of sa1a + pva after testing.....	40
Figure 61. Load-midspan deflection response for sa2a and sa2a+pva.....	41
Figure 62. Final view of sa2a after testing	41
Figure 63. Final view of sa2a+pva after testing.....	41
Figure 64. Load-midspan deflection response for sa3a and sa3a+pva.....	42
Figure 65 . Final view of sa3a after testing.	42
Figure 66. Final view of sa3a+pva after testing.....	43
Figure 67. Load-midspan deflection response for sa4a and sa4a+pva.....	44
Figure 68. Final view of sa4a after testing.	44
Figure 69. Final view of sa4a+pva after testing.....	45
Figure 70. Maximum loads for four-point bending tests.....	46
Figure 71. Maximum moments for four-point bending tests.....	46
Figure 72. Maximum moments for steel fiber only specimens.	47
Figure 73. Maximum moments for specimens with pva fibers.	48
Figure 74. Compression strength for concrete mixes.....	50

LIST OF TABLES

<u>Table</u>	<u>Page</u>
Table 1. Types of fiber reinforcement (kaur, 2017).....	5
Table 2. The figures, the properties and the usage of each type of hooked ended steel reinforcement.....	7
Table 3. Properties of the steel fiber used.....	15
Table 4. The properties of the pva fiber:	16
Table 5. Concrete mix content	17
Table 6. Specimens fiber content.....	18
Table 7. Maximum load and moments for three-point bending tests.....	37
Table 8. Maximum total load and moments for four-point bending tests.....	45
Table 9. Cylinder compressive strengths for sa1 mix.	48
Table 10. Cylinder compressive strengths for sa2 mix.	49
Table 11. Cylinder compressive strengths for sa3 mix.	49
Table 12. Cylinder compressive strengths for sa4 mix.	50

CHAPTER 1

INTRODUCTION

Reinforced concrete is composite material, which can be considered as one of the most universally used materials in the contemporary construction. Concrete is known as an “artificial stone “that is formed by mixing cement, sand and aggregates by water. Its benefits became more favored after the invention of the Portland cement by the end of the 19th century.

It’s stiffness and compressive strength simultaneously with a low cost made concrete a very valuable and useful material. In addition, durability, economy, freeze and thaw resistance and shrinkage are considered as characteristics of the concrete.

Although concrete is characteristically very robust material, the opposite is true for tensile and flexure loading. To increase the tensile resistance of concrete, reinforcing is used. Reinforcement can be done with different methods: the basic and traditional one is by adding steel bars. Alternatively, mixing concrete with randomly dispersing fibers during the mixing process is another reinforcing method. In this case, one type or a mix of different types of fibers can be used. The obtained mix is called fiber reinforced concrete or hybrid fiber reinforced concrete for a mix of different types of fibers. This mixture permits us to profit from the high compression strength of the concrete and to surpass the limited tension and flexural resistance.

The use of the fiber mixing method was invented and used for the first time at least 3500 years ago. At that time in AqarQuf near Baghdad, a tower of 57 meter in height was build using sun-baked bricks reinforced with straw. Nowadays, fiber reinforced concrete is widely used in the building industry and the airport pavements.

During the last two decades, extensive research has been done to improve information and applicable uses of the fiber reinforced concrete. On the other hand, it appears that more knowledge still is required especially about hybrid fiber reinforced concrete and contributions of different types of fibers to the tensile and flexural behavior of concrete.

Bending tests are one of the common types of tests that are employed for

investigating the efficiency of fibers. Three-point bending tests, where a single concentrated load is applied at the midspan of a simply supported prismatic beam, or four-point bending tests, where two equal concentrated forces are applied at third points on a simply supported prismatic beam are the most common tests performed by researchers in this area. A characteristic load-deflection curve that can be obtained from such tests for fiber reinforced concrete can be seen in Figure 1. As seen, fiber reinforced concrete considerably increases the ductility of these members, of which otherwise would fail abruptly in a brittle manner.

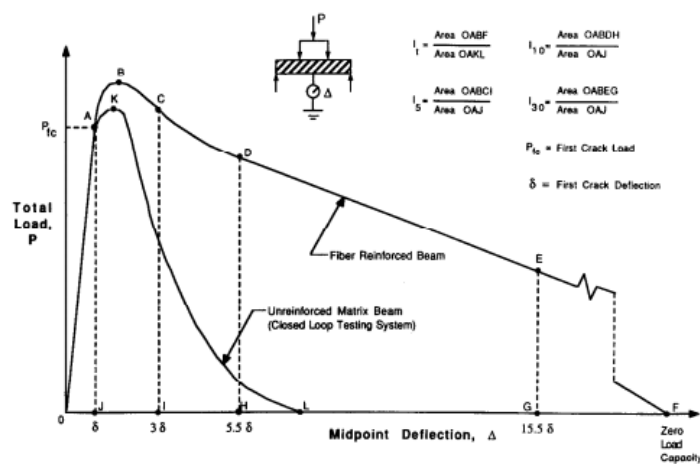


Figure.1. Typical load-deflection behavior of fiber reinforced concrete beams (ACI 54, 1999)

1.1 Objective

This study is conducted to improve our knowledge on the use of hybrid reinforced fiber concrete. Performance of hybrid reinforced concrete beams, where steel and polyvinyl alcohol (PVA) fibers are used in the same mix, were investigated under three- and four-point bending tests. Effects of fiber hybridization on the bending behavior were also investigated through comparison of the behaviors between steel fiber reinforced and hybrid fiber reinforced concrete beams with identical geometry.

1.2 Thesis Organization

Chapter 2 presents a brief summary of the previous researches and experimentation done on the topic of hybrid reinforced concrete, within the scope of this thesis.

Chapter 3 introduces the experimental work done in the laboratory on a number of beams with different steel and PVA fibers.

Chapter 4 presents the results obtained from tests given in the previous chapter. Comparisons and discussions about the test results are given in this chapter.

Chapter 5 outlines the fundamental conclusions achieved from this study.

CHAPTER 2

LITERATURE REVIEW

2.1 Introduction

Many kinds for construction materials has been used for construction, but still concrete is the most used material for the modern buildings .Due to the profuse use of this material mechanical properties of concrete have been thoroughly studied. The high stiffness and the good compression strength added to the low cost can define the principal characteristic of the concrete. Concrete normally used with steel bars in reinforced concrete to overcome the low tensile strength of concrete. Recently, steel or synthetic fibers are also used to improve the tension performance of concrete, which is called fiber reinforced concrete.


2.2 Types of Fiber Reinforcement

On the ground that, using fiber reinforced concrete is a very useful and advantageous method, a number of types of reinforcement fiber where invented and used.

Depending on the difference in the sizes, shapes, material and usage, concrete fiber reinforcing can be mainly divided on the following types (Table1):

- Steel fiber reinforced concrete (SFRC): It is responsible to augment the concrete properties: flexural and fatigue strength.
- Glass fiber reinforced concrete (GFRC): It is used mostly for the exterior buildings, facades panels and for the architectural precast concrete.
- Synthetic fiber reinforced concrete (SNFRC): This type of fiber is more durable comparing with other fibers.
- Natural fiber reinforced concrete (NFRC): It can be treated as the most economic fiber Also it does not require a big amount of energy.

Table 1: Types of fiber reinforcement (Kaur, 2017)

 <p data-bbox="427 629 836 663">Figure 2: Steel fiber (Kaur, 2017)</p>	 <p data-bbox="959 629 1367 663">Figure 3: Glass fiber (Kaur, 2017)</p>
<p data-bbox="448 689 810 723">Steel fiber reinforced concrete</p>	<p data-bbox="979 689 1351 723">Glass fiber reinforced concrete</p>
 <p data-bbox="405 1167 861 1200">Figure 4: Synthetic fiber (Kaur, 2017)</p>	 <p data-bbox="954 1167 1378 1200">Figure 5: Natural fiber (Kaur, 2017)</p>
<p data-bbox="427 1225 836 1258">Synthetic fiber reinforced concrete</p>	<p data-bbox="970 1225 1362 1258">Natural fiber reinforced concrete</p>

2.3 Properties Of The Used Fibers:

Two types of fibers were used in this study: Steel fibers and Polyvinyl Alcohol Fibers (PVA). In this section, their properties are summarized.

2.3.1 The Steel Fiber:

Steel fibers are the most used fiber for the reinforcement. Main properties of the steel fibers can be summarized as below (Kaur, 2017):

- Their diameter is between 0.25 and 0.75 mm.
- They are responsible to augment concrete properties: Flexural and fatigue

strength.

- They have a very high tensile strength.
- They help to reducing cracking.
- They protect against severe cold.
- They perform better if they are used with normal steel reinforcement or with other types of fibers.
- They can be used for the overlays of road, bridge decks, thin shells and plates.

Common steel fiber types are shown in the Figure 6:





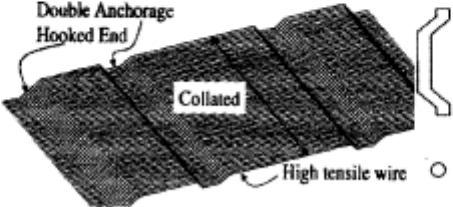

Straight slit sheet or wire	Deformed slit sheet or wire	Machined chips
 <p data-bbox="421 1084 536 1111">□ or ○</p>	 <p data-bbox="667 1084 1027 1111">□ ○ ○ or ◡</p>	 <p data-bbox="1174 1084 1230 1111">◡</p>
Melt extract	Hooked-end wire (Crimped)	Enlarged-end
 <p data-bbox="472 1435 512 1462">◡</p>		

Figure 6 : Types of fiber reinforcement (Kaur, 2017)

- Straight slit sheet or wire: It can have rectangular or circular sections.
- Deformed slit sheet or wire: It can have a rectangular, circular or semicircular section.
- Machined chips: It can have semicircular sections.
- Melt extract: It has a semicircular section.
- Hooked-end wire (crimped): This type have circular sections.

- Enlarged end.

The type of steel fiber used in this study is the hooked ended steel fibers that can be specified with the aspect ratio and the length of the fiber. The hooked ended steel fibers provided under the brand Dramix™ are divided into three types named as: 3D , 4D and 5D (“Bekaert,” n.d.) (Figure 7)

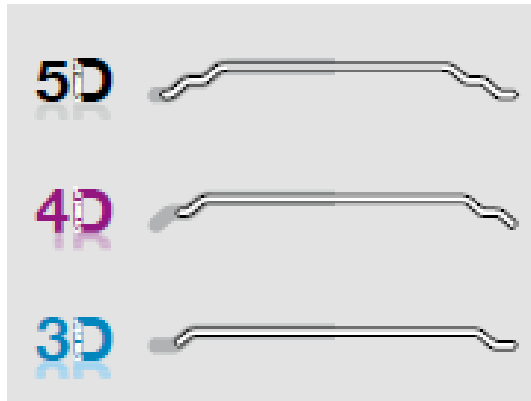





Figure 7: Types of hooked ended steel reinforcement (“Bekaert,” n.d.)

The figure, the properties and the usage of each type of hooked ended steel reinforcement can be resumed in the following table (Table 2):

Table 2: The figures, the properties and the usage of each type of hooked ended

steel reinforcement

3D	4D	5D
 <p data-bbox="288 524 616 589">Figure 8:3D hooked ended steel fiber (“Bekaert,” n.d.)</p>	 <p data-bbox="667 524 994 589">Figure 9: 4D hooked ended steel fiber (“Bekaert,” n.d.)</p>	 <p data-bbox="1046 524 1374 589">Figure 10:5D hooked ended steel fiber (“Bekaert,” n.d.)</p>
Properties		
<p data-bbox="272 667 630 770">It provides the time saving and cost efficient High durability</p>	<p data-bbox="655 651 1005 786">It provides the highest serviceability. It effects cracks between 0.1 and 0.3 mm</p>	<p data-bbox="1031 651 1398 786">It provides the best performance Non deformable hook Ductile wires.</p>
Usage		
<p data-bbox="272 864 472 967">Jointed floors Hard standings Bonded overlays</p>	<p data-bbox="655 853 954 1012">Slab tracks Secondary reinforcement Concrete roads Underwater concrete Heavy duty pavement</p>	<p data-bbox="1031 853 1278 1012">Structural rafts Bridges Clad racks Structural floors Pile supported floors</p>

2.3. 2 Properties Of The Steel Fiber Reinforcement:

The report by the ACI committee 544 (ACI 544, 1999) provide extensive information about the mechanical properties of steel fiber reinforcement that is affected mainly by the dimensions of the fibers , the quantity , the geometry , geometry of the specimens and preparation method .

- **Compressive Behavior:**

The report by the ACI committee 544 discuss the effect of steel fiber on the compressive strength of concrete. The effect can be considered as not stable and vary between insignificant to slight.

The Figure 11 presents typical stress-strain curves for steel fiber reinforced concrete in compression for different volume fractions. It can be concluded that increase in the volume of the steel fiber in the mix design can affect noticeably the stress strain curve and improve the maximum strain capacity.

The Figure 12 gives more information about the influence of the aspect ratio of

fibers on the stress-strain curve. It can be concluded that the augmentation of the length-diameter ratio affects the compressive stress-strain curve especially in the descending part of the graph.

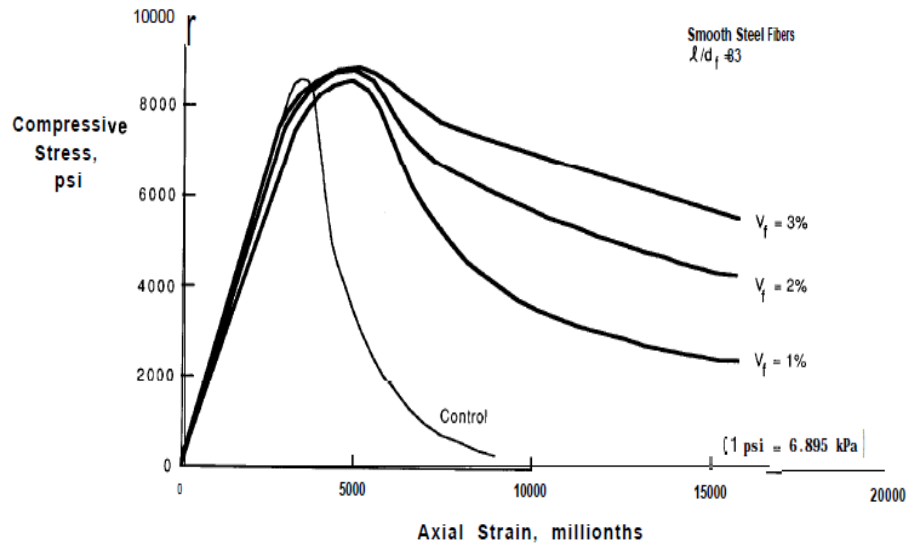


Figure 11: Influence of the volume fraction of fibers on the compressive stress-strain (ACI 544, 1999)

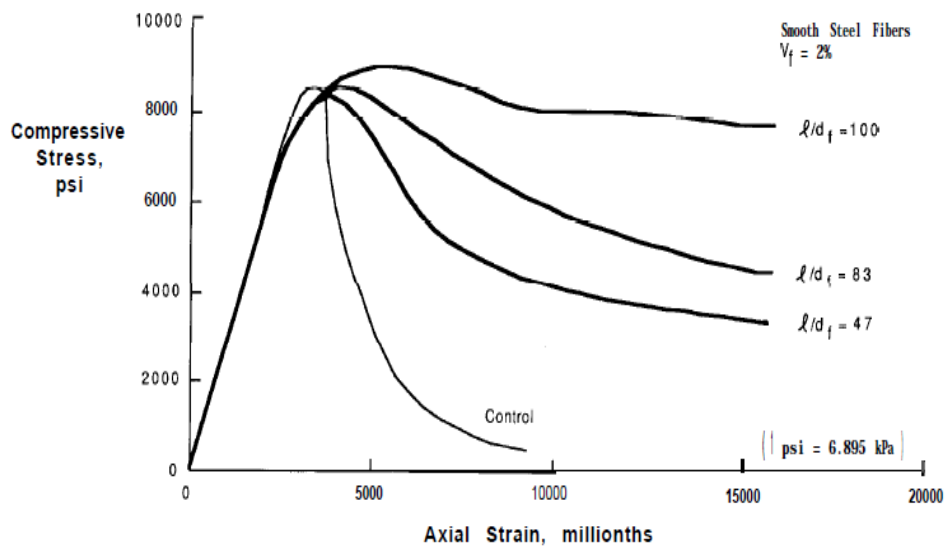


Figure 12: Influence of the aspect ratio of fibers on the stress-strain curve (ACI 544, 1999)

- **Direct tension behavior:**

The report by the ACI committee 544 (ACI 544, 1999) discussed also the direct tension behavior of steel fiber reinforced concrete. The stress strain curve is based mainly on the size of the specimen, the method of testing, the stiffness, the length of the

gage and the type of the cracks.

The direct tension stress strain curves of the steel fiber reinforcing can be presented in the following Figure 13.

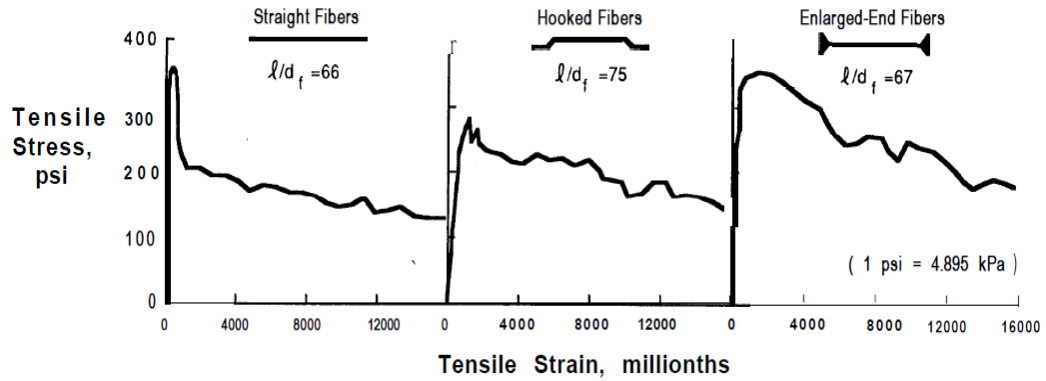


Figure 13: Stress-strain curves for steel fiber reinforced mortars in tension (ACI 544, 1999)

The curves can be divided on two parts:

- The first part that is the escalate part that is so similar to the curve of the mortar not reinforced.
- The second part that is the drop part is depending mainly on the parameters of the fibers.
- **The flexural strength:**

The steel fiber has more effect on the flexural strength of concrete than on the direct tension and compression.

Figure 14 presents typical load-deflection response of a steel fiber reinforced beam under bending. As seen in the figure, steel fibers significantly enhance the post-peak ductility of the beams.

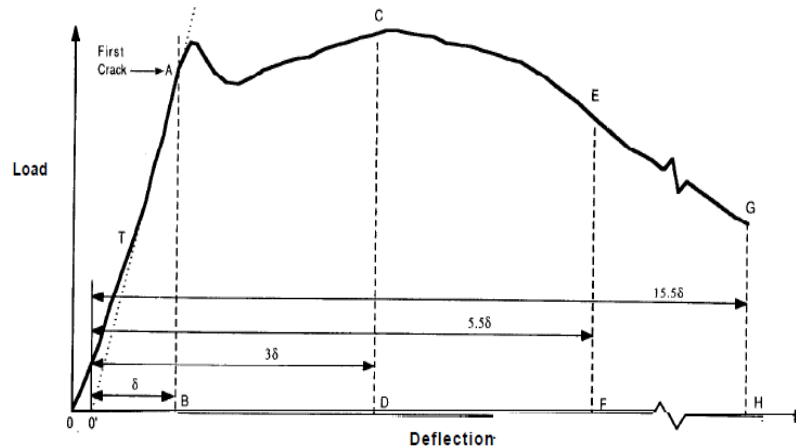


Figure 14: Characteristics of the load-deflection curve. (ACI 544, 1999)

2.3.3 Polyvinyl Alcohol Fibers (PVA):

The polyvinyl alcohol fibers (PVA) are a type of synthetic fibers that is frequently used in concrete. Main properties of the synthetic fibers are summarized below (Kaur and Talwar 2017):

- It helps to improve the concrete performance.
- This type of fiber is more durable compared to other fibers.
- For the hardened concrete, this type of fibers is used to augment its strength.
- For the case of a semi-hardened concrete, this type of fibers is used to control the cracks.
- Since synthetic fibers do not expand in heat and contract at low temperatures, it helps to prevent cracking in such situation.

The most used synthetic fibers used are: carbon, nylon, polyester, polypropylene and polyethylene.

2.3.4 Effects of Fibers on the Flexural Behavior of Concrete Beams:

There are numerous studies conducted on the bending behavior of fiber reinforced concrete. Majority of studies involved three-point or four-point bending tests of beams.

In the study by (Hameed et al. 2013), A number of beams were tested under three-point bending test. Two types of fibers were used, amorphous metallic fibers and carbon steel hooked-end fibers. It was concluded that the ultimate flexural strength of the beam was increased by 4 to 7.5% when steel fiber reinforcement was used. In addition, evolutions of the cracks were greatly affected. It was found that the improvement in the flexural strength of the FRC beams greatly depends on physical and mechanical properties of metallic fibers. Addition of metallic fibers permits a significant reduction in the crack width and the deflection of the reinforced concrete beams.

The geometry of the specimens as well as the fiber properties are important parameters that affect the flexural strength and cracking patterns of fiber reinforced concrete beams. Experimental work by (Maalej, Hashida, and Li 2011) showed that increasing the beam depth decreased its flexural strength (Figure15).

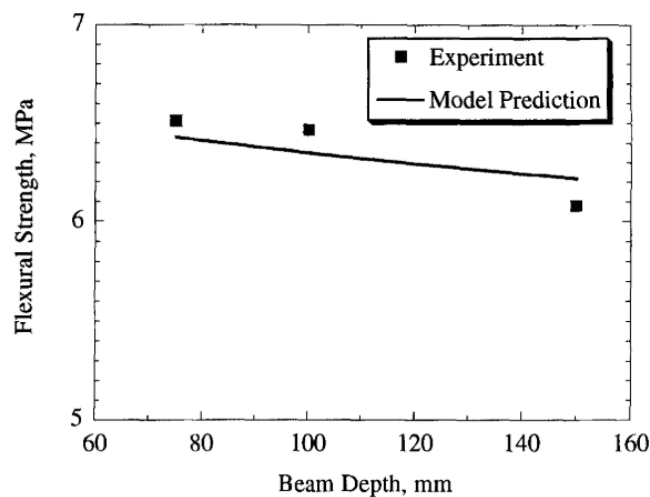


Figure 15: Effect of beam depth on the flexural strength of the steel fiber reinforced concrete. (Maalej, Hashida, and Li 2011).

The modeling of steel fiber reinforced concrete under flexure is presented by (Singh 2015) where parametric studies were executed by using of an analytical model. It was found that the type and dimensions of steel fibers influence the flexural behavior of the beams differently. Long fibers can guarantee a better performance compared to short fibers and they affect the width of the cracks.

The polyvinyl alcohol (PVA) fibers also have a significant effect on the bending strength of concrete beams.

The study by (Zhang et al. 2019) showed that PVA fibers were able to improve the flexural strength of concrete beams (Figure16). As they also decrease crack propagation by decreasing stress concentration at the tip of the crack as shown in Figure 17 where P0.6, P0.9, P1.2 and P1.5 designed the specimens with 0.6%, 0.9%, 1.2% and 1.5% volumetric ratio of PVA fibers in concrete, respectively.

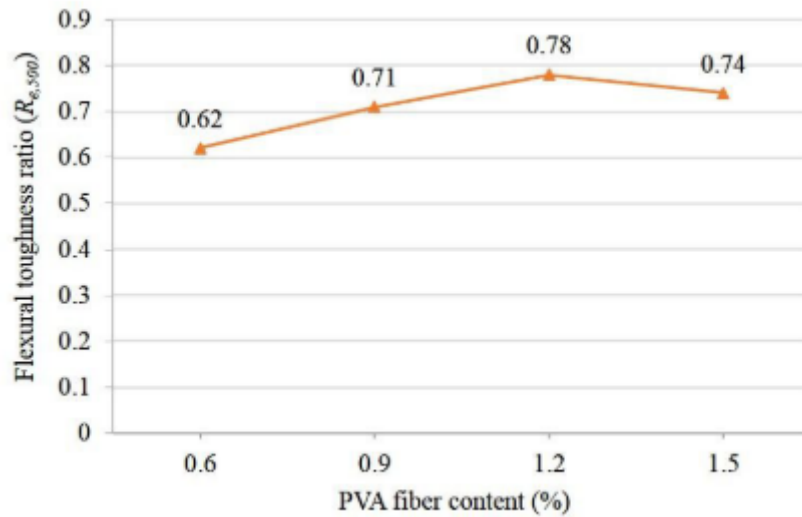


Figure 16: Flexural toughness ratio of the composites with different PVA fiber Contents (Zhang et al. 2019).

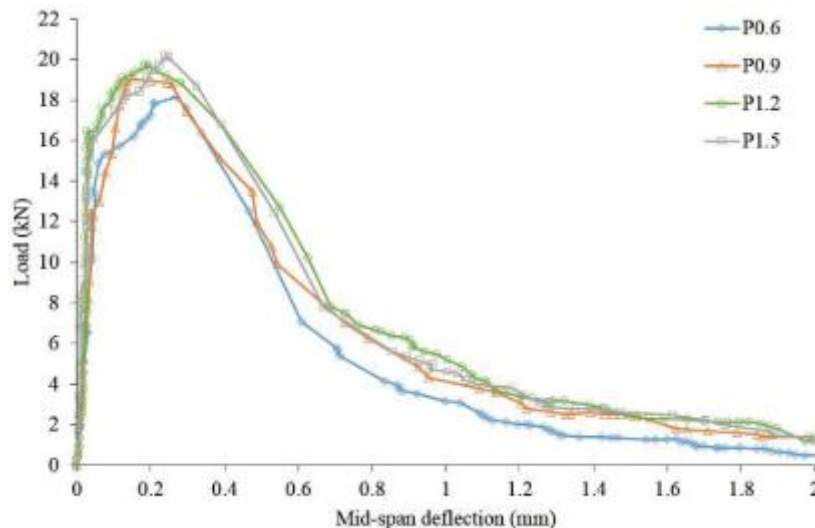


Figure 17: Load vs. mid-span deflection for composites with different PVA contents (Zhang et al. 2019).

As it is shown, both steel fibers and PVA fibers have a strong effect on the flexural behavior of concrete beams. There have been studies in the literature using both types of fibers in the same mix and taking advantage of their individual contributions to the behavior, which is commonly referred as hybrid fiber reinforced concrete.

(Chasioti and Vecchio 2017) performed tests on beam and direct tension specimens using hybrid fiber reinforced concrete. They found that long fibers increase peak bending stress and fracture toughness due to their pullout resistance, where as short fibers effect dilatation of concrete.

(Alberti, Enfedaque, and Gálvez 2017) performed three-point bending tests on hybrid fiber reinforced concrete beams. They concluded that the ductility and residual strength were improved when both types of fibers were used compared to the case of use of single fibers.

(Abadel 2016) tested beams with different volume fraction of hybrid fibers under three-point bending. The load displacement response has showed that the addition of hybrid fibers in concrete improved the flexural strength of the concrete.

(Caggiano et al. 2016) focused on the post cracking response of steel and polypropylene hybrid fiber reinforced concrete beams. A number of beams were tested with the same total fiber volume fraction but with different volume combination for each type of fiber. Results showed that using steel fibers and the polypropylene fibers in the same mix is a very effective method to improve the post-cracking behavior of concrete in compression and in bending. They found that a higher amount of steel fibers in the mixture can be more advantageous. On the other hand, the mixtures with higher amount of polypropylene can result a general reduction in the strength and toughness.

CHAPTER 3

EXPERIMENTAL WORK

An experimental study was conducted to determine the effect of steel fiber types and fiber hybridization on the flexural behavior of one-way members. Details of the test program are given in this chapter.

3.1. Materials And Mix Proportions:

In the aim of obtaining the flexural behavior of a hybrid fiber reinforced concrete, a number of specimens with different mix designs were tested. These mix designs were taken from an extensive study by (Paper et al. 2018) investigating the performance of numerous mix designs for hybrid fiber reinforced concrete.

CEM I 42.5 Portland cement was used in the study, which is pure Portland cement without any additives.

Two types of aggregates were used. Fine aggregates had a specific gravity of 2.59 and an absorption capacity of 2.67%, whereas the coarse aggregates had a maximum diameter of 12 mm, a specific gravity of 2.56 and an absorption capacity of 1.37%.

Class-F fly ash, with a specific gravity of 2.61 and Blaine finesse of 290m²/kg was also used in the mix, forming roughly 4% of the total mixture volume. A polycarboxylic super plasticizer (Master Glenium 21) was used to increase the workability. Three types of steel fibers were used, all with Dramix™ brand (Figure 18). Properties of these fibers are given in Table 3.

Table 3: Properties of the steel fiber used.

Reference	35 /45 3D	65/60 3D	65/60 5D
Type	hooked	hooked	Hooked
Length (mm)	45	60	60
Diameter (mm)	0.78	0.92	0.92
Aspect ratio (mm)	35	65	65



Figure 18: The used steel fiber.

Polyvinyl Alcohol (PVA) fibers used in the mix were Kuralon K-II RECS 15/8mm brand (figure 19) with the properties given in the Table 4:

Table4 : The properties of the PVA fiber:

Length (mm)	8
Diameter (μm)	40
Specific gravity	1.3
Nominal strength (MPa)	1610
Apparent strength (MPa)	1092
Ultimate Strain	6%
Young modulus (GPa)	42.8



Figure 19: The used PVA fiber.

Eight specimens were casted for the experimental program. Same concrete mix was used for all specimens (Table 5). Specimens were cast in pairs of four different steel fiber contents. One of the two specimens with the same steel fiber content had additional PVA fibers. The fiber content for each type of each specimen is resumed in the table 6 where the last casted specimen was addressed to be a control specimen where it does not contain any reinforcement fibers.

Table 5: Concrete Mix Content

Material	Weight (kg/m ³)
Cement	272
Fly ash	320
Water	240
Course aggregates	672
Fine aggregates	624

Table 6:Specimens fiber content.

Specimen	Steel Fiber Type	Steel Fiber Content (% Volume)	PVA Fiber Content (% Volume)
SA1	Dramix35/45 3D	0.75	0
SA1+PVA	Dramix35/45 3D	0.75	0.25
SA2	Dramix 65/60 3D	0.75	0
SA2+PVA	Dramix 65/60 3D	0.75	0.25
SA3	Dramix 65/60 5D	0.75	0
SA3+PVA	Dramix 65/60 5D	0.75	0.25
SA4	Dramix 65/60 3D	1.25	0
SA4+PVA	Dramix 65/60 3D	1.25	0.25
Plain	-	-	-

3.2. Specimen Preparation:

Concrete mixture was prepared, molded, and cured at the Izmir Institute of Technology laboratories.

Coarse aggregates were sieved with 12 mm sieve to obtain proper gradation. All mixture components were carefully measured, weighed. Mixing is done in a mixer with maximum capacity of 100 liters (Figure 20).Mixing started by the aggregates, followed by cement and fly ash, and lastly steel fibers and PVA fibers. During these steps, water with diluted super plasticizer was continuously added.



Figure 20: Rotation drum mixer

After mixing, concrete was cast in oiled wood formworks as shown in the Figure 21, with the dimensions of 2.5*0.5*0.05 m. Mechanical vibration was applied to assure the homogeneity of the concrete.

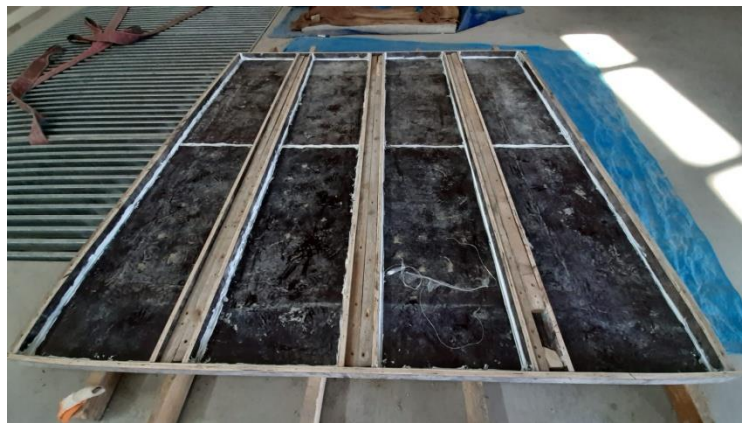


Figure 21: Formworks

Specimens were removed from the formworks after 24 hours, and they were covered with plastic bags and burlap to sustain humidity for curing.

Specimens were cured for 90 days, during which they were daily moisturized.

3.3. Testing Procedure

Specimens were tested under three-point and four-point loading. Details of the test setup and instrumentation are presented in the following sections.

3.3.1. Three-point Bending Tests

Test setup used in three-point bending tests is presented in Figure 22. Specimens, with the dimensions of $2.5 \times 0.5 \times 0.05$ m were placed on a roller support and a pin support, forming simply supported conditions (Figure 24). Load was applied by a displacement controlled hydraulic actuator at the midspan, through a 20 mm diameter steel cylinder, forming a linear load distribution. Load was applied at a constant rate of 1.5 mm/minute.



Figure 22: Bending test mechanism

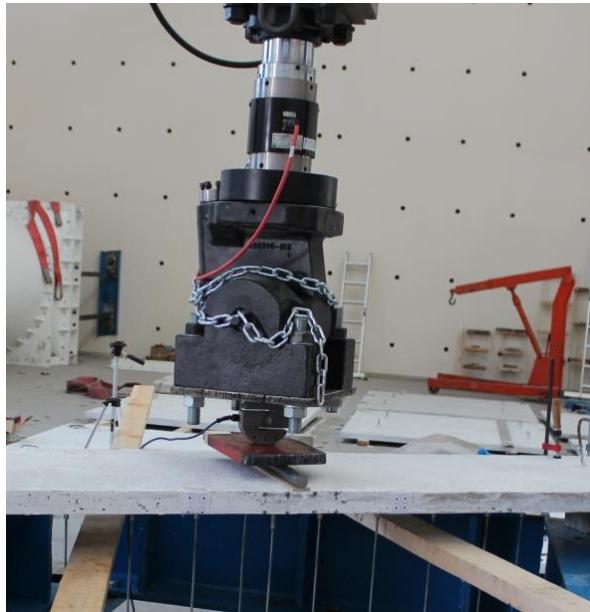


Figure 23: Loading point at the midspan.

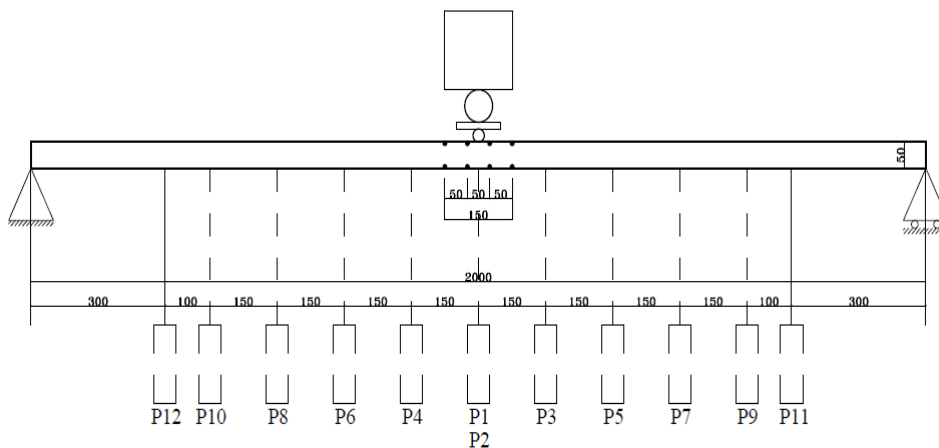


Figure 24: Test setup for three point bending

Specimens were instrumented with 12 linear resistive position transducers (RLPT) attached to the bottom of the specimens to measure the displacements (Figure 25 and 26). Two RLPT's were placed at the midspan to obtain a better midspan measurement. A load cell was placed under the loading head of the hydraulic jack to measure the applied load.



Figure 25: Linear resistive position transducer.

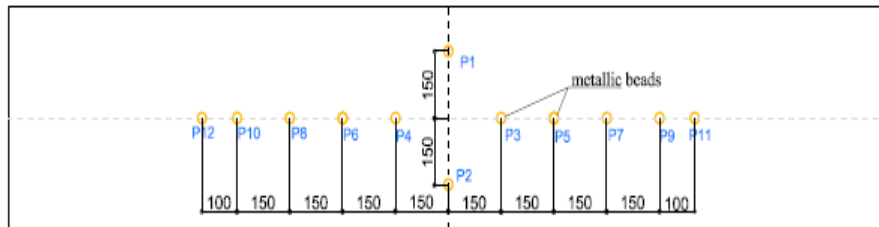


Figure 26: The disposition of linear resistive position transducers.

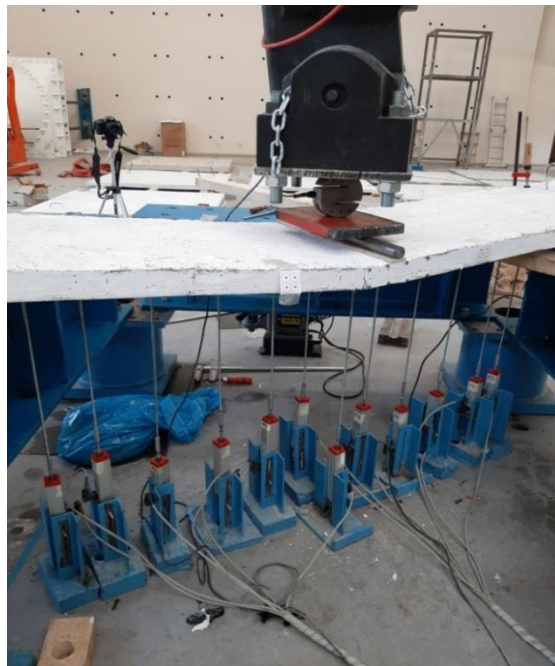


Figure 27: The disposition of the linear resistive position transducer after deflection.

To measure the crack opening on the beam, eight metallic beads were fixed to one side of the specimen by epoxy at the midspan (Figure 28) and change in distance between the beads were measured manually with a high-precision digital movement gauge . Approximate placements of the beads are presented in Figure 29, whereas actual distances were measured before the tests by using the digital gauge. Measurements were taken after cracking by pausing the load and manually taking the measurements at certain displacement intervals.

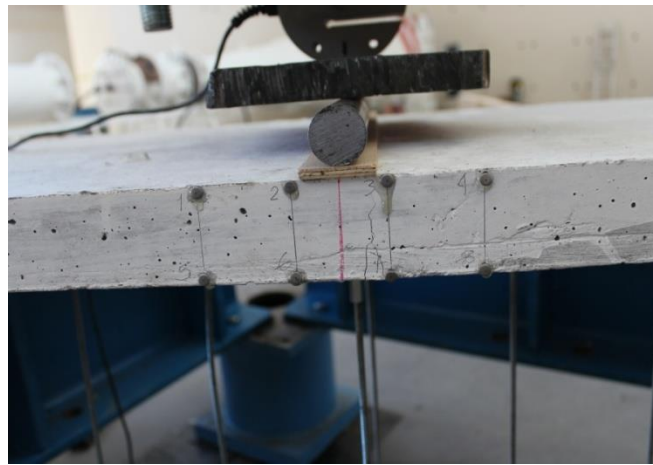


Figure 28: The distribution of the beads for the three point bending test.

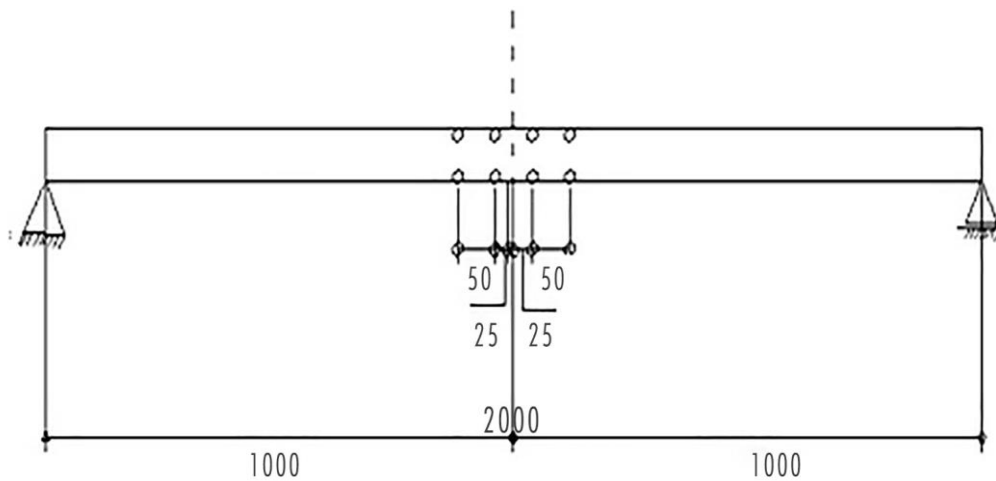


Figure 29: Placement of beads for three-point bending test.

the displacements. Similar to three-point tests, metallic beads were used to measure the crack opening on the beam. Beads in these tests were placed slightly differently to catch the cracks in the constant moment region (Figure 32). Approximate placements of the twelve beads are presented in Figure 33.



Figure 32: Beads for the four-point bending test.

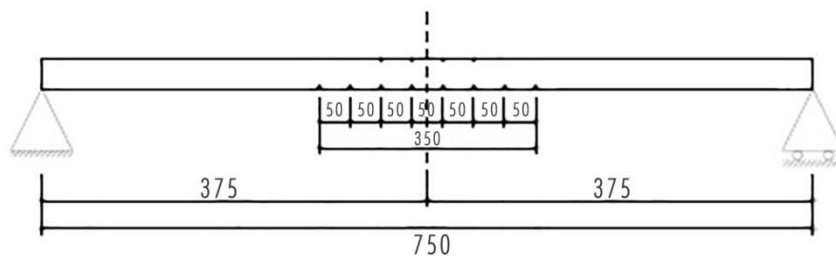


Figure 33: Placement of beads for four-point bending tests.

3.3.3. The Compression Tests:

For each mix, cylinder specimens were taken to obtain the compressive strength (Figure 34). Two types of cylinders were used: 100 mm diameter and 200 mm height, and 150 mm diameter and 300 mm height. For each mix design three cylinders were tested with both sizes. Three samples were taken from the mix for each time before addition of any fibers, after adding steel fibers and after adding PVA fibers.

Cylinders were tested according to the standard test method for the compressive strength of the cylindrical concrete specimens ASTM C39 at the same period when the bending tests were executed using a digital compression machine (Figure 35).



Figure 34: The cylinders ready to be tested.



Figure 35: The digital compression machine.

CHAPTER 4

TEST RESULTS AND DISCUSSION

All tests were performed at the Structural Laboratory of Izmir Institute of Technology. This chapter summarizes the results obtained.

4.1. Three-point Bending Tests

The specimens with the dimensions of $2.5 \times 0.5 \times 0.05$ m were tested under a three-point bending. Results are given in following sections.

4.1.1. SA1 And SA1+PVA

Load- midspan deflection response of SA1 and SA1+PVA is presented in Figure 36, photos of specimens at the final stage of the testing are given in Figure 37 and 38 and the sections photos are presented in the Figure 39 and 40.

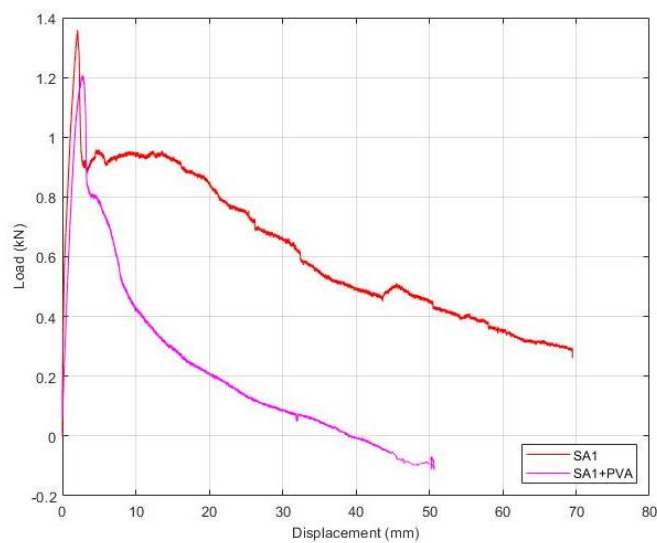


Figure 36: Load-midspan deflection response for SA1 and SA1+PVA

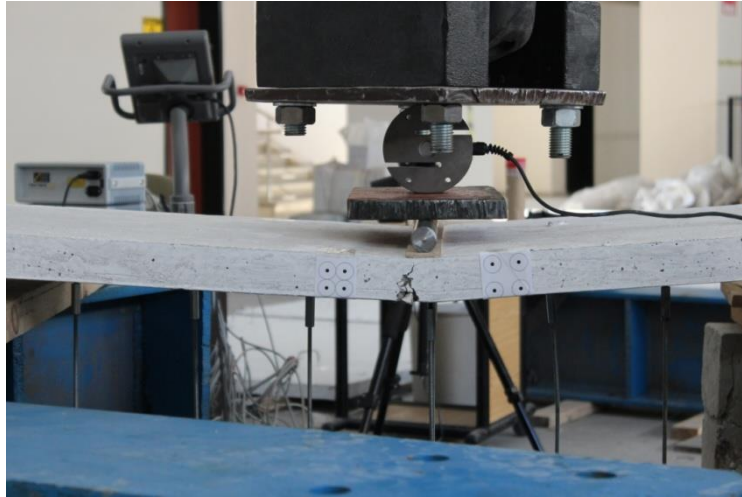
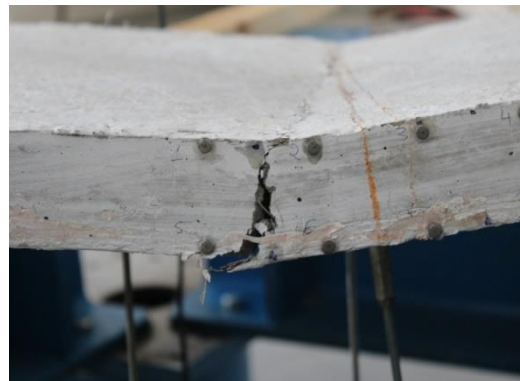


Figure 37: Final view of SA1 after testing



(a) Bottom view



(b) Side view

Figure 38: Final view of SA1+PVA after testing.



Figure 39: Section Photo of SA1



Figure 40: Section photo of SA1+PVA

Dramix 35/45 3D steel fibers were used for these specimens. Specimen with only steel fibers, SA1, sustained a maximum load of 1.35 kN, whereas SA1+PVA sustained a lower level of load of 1.20 kN, corresponding to 0.72 kN.m and 0.65 kN.m maximum moment capacities, respectively. As seen in figure, both specimens failed due to a single crack at the midspan. Load dropped abruptly in both specimens after the first crack. Although they had very close maximum load capacity, SA1 sustained higher levels of load after initial cracking. Addition of PVA had an adverse effect for this shorter steel fiber.

4.1.2. SA2 And SA2+PVA

Load-midspan deflection responses of SA2 and SA2+PVA are presented in Figure 41, photos of specimens at the final stage of the testing are given in Figure 42 and 43 and the sections photos are presented in the Figure 44 and 45.

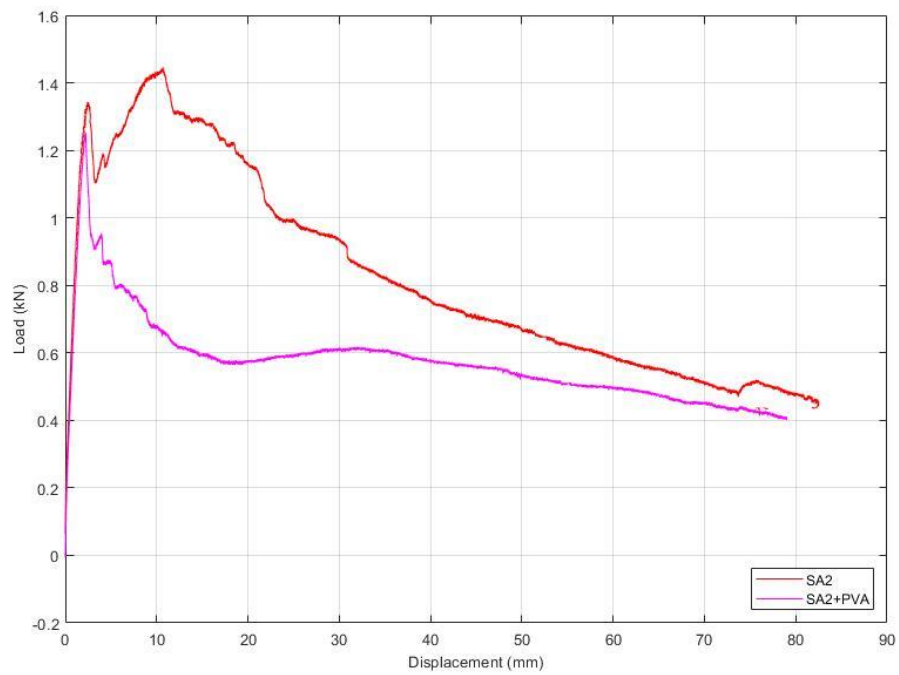
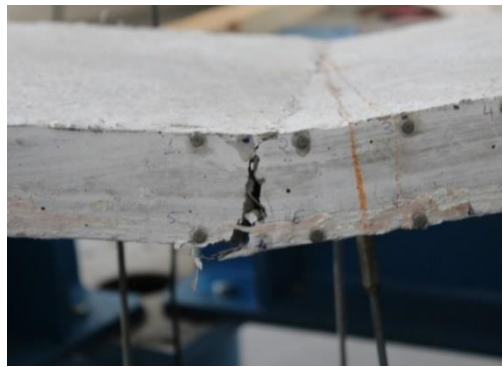


Figure 41: Load-midspan deflection response for SA2 and SA2+PVA.



(a) Bottom view



(b) Side view

Figure 42: Final view of SA2 after testing



Figure 43: Final view of SA2+PVA after testing



Figure 44:Section Photo of SA2



Figure 45: Section Photo of SA2+PVA

Single hook-end Dramix 65/60 3D steel fibers were used for these specimens. Specimen with only steel fibers, SA2, sustained a maximum load of 1.45 kN, whereas SA2+PVA sustained a lower level of load of 1.25 kN, corresponding to 0.78kN.m and 0.67kN.m maximum moment capacities, respectively. As seen in figure, both specimens failed due to a single crack at the midspan. However, in SA2, cracking occurred slightly at an inclined angle with respect to middle axis. Load dropped abruptly in both specimens after the first crack, which occurred around very close midspan displacement. However, for SA2, load started to rise again and reached its maximum at a higher displacement than SA2+PVA. Consequently, SA2 sustained higher levels of load after initial cracking. Addition of PVA had an adverse effect for this mix.

4.1.3. SA3 And SA3+PVA

Load- midspan deflection responses of SA3 and SA3+PVA are presented in Figure 46, photos of specimens at the final stage of the testing are given in Figure 47 and 48 and the sections photos are presented in the Figure 49 and 50.

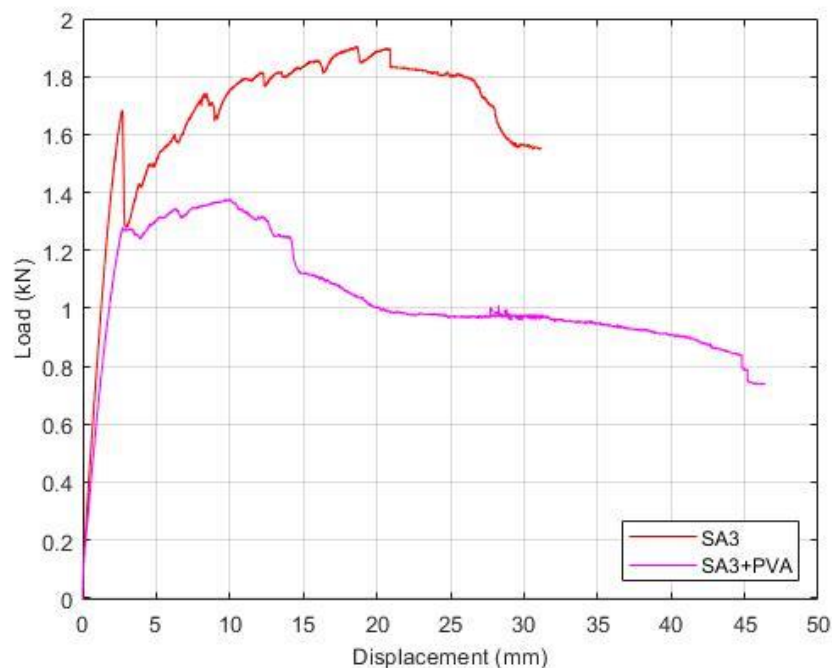


Figure 46: Load-midspan deflection response for SA3 and SA3+PVA



(a) Bottom view



(b) Side view

Figure 47: Final view of SA3 after testing.



Figure 48: Final view of SA3+PVA after testing



Figure 49: Section Photo of SA3



Figure 50: Section Photo of SA3+PVA

Double hook-end Dramix 65/605D steel fibers were used for these specimens. Specimen with only steel fibers, SA3, sustained a maximum load of 1.91 kN, whereas SA3+PVA sustained a lower level of load of 1.38 kN, corresponding to 1.02kN.m and 0.74kN.m maximum moment capacities, respectively. As seen in figure, both specimens failed due to a single crack at the midspan. Load dropped abruptly in SA3 after the first crack; however, it started to rise again and reached its maximum at a higher displacement than SA3+PVA. Load for SA3+PVA had a slight rise after cracking but then load had a steady decline.

4.1.4. SA4 And SA4+PVA

Load- midspan deflection responses of SA4 and SA4+PVA are presented in Figure 51, photos of specimens at the final stage of the testing are given in Figure 52 and 53 and the sections photos are presented in the Figure 54 and 55.

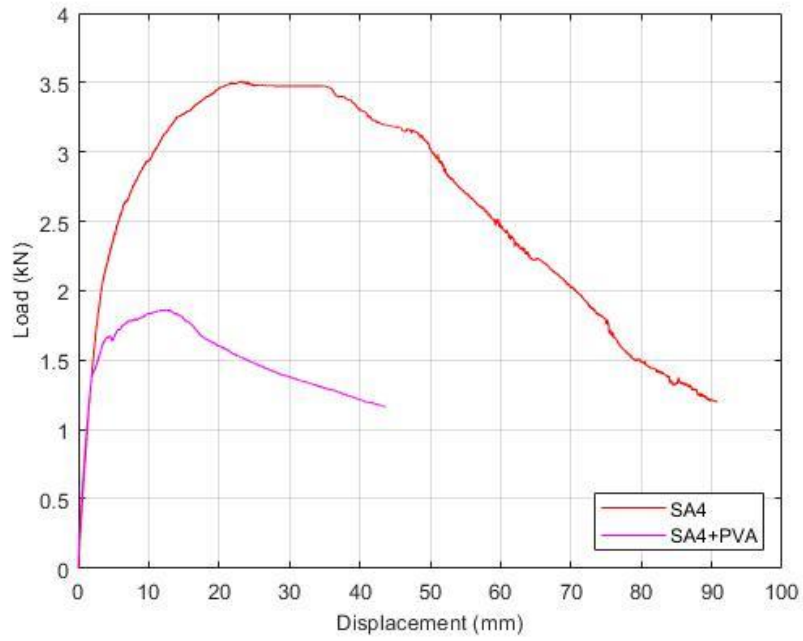


Figure 51: Load-midspan deflection response for SA4 and SA4+PVA.



(a) Bottom view



(b) Side view

Figure 52: Final view of SA4 after testing.



(a) Side view



(b) Bottom view

Figure 53: Final view of SA4+PVA after testing.



Figure 54: Section Photo of SA4



Figure 55: Section Photo of SA4+PVA

Single hook-end Dramix 65/603D steel fibers were used with a higher percentage for these specimens. Specimen with only steel fibers, SA4, sustained a maximum load of 3.51 kN, whereas SA4+PVA sustained a lower level of load of 1.86 kN, corresponding to 1.89kN.m and 1.00kN.m maximum moment capacities, respectively. As seen in figure, both specimens failed due to a single crack at the midspan. Load-deflection curves for both specimens had a smooth parabolic shape. Unlike others, cracking did not induce a sudden drop in these specimens but caused a steady decrease in stiffness instead. SA4 sustained considerably higher level of loads and reached higher level of displacements compared to SA4+PVA. Addition of PVA had a serious adverse effect for this mix.

4.1.5. Discussion of Results For Three-point Bending Tests

Maximum load and moments obtained from three-point tests are summarized in Table 7, Figure 56 and Figure 57.

Table7: Maximum load and moments for three-point bending tests

Specimen	Maximum Load (kN)	Maximum Moment (kN.m)
SA1	1.35	0.72
SA1+PVA	1.20	0.65
SA2	1.45	0.78
SA2+PVA	1.25	0.67
SA3	1.91	1.02
SA3+PVA	1.38	0.74
SA4	3.51	1.89
SA4+PVA	1.86	1.00

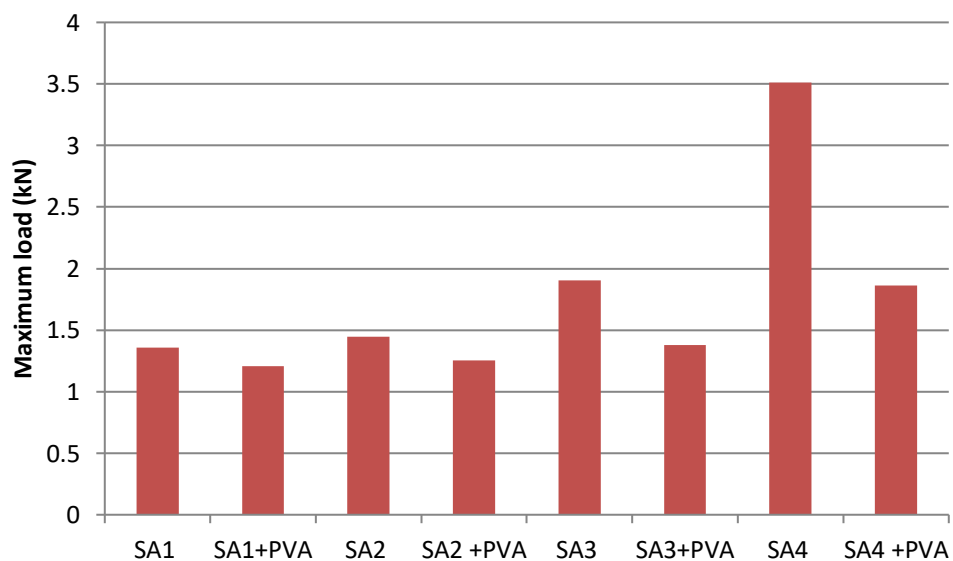


Figure 56:Maximum loads for three-point bending tests.

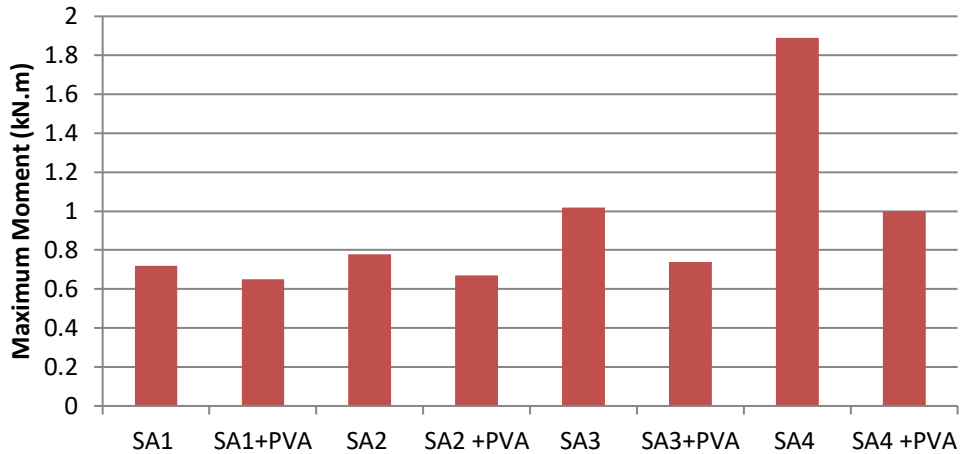


Figure 57: Maximum moments for three-point bending tests.

As seen from test results, highest load capacity was obtained from SA4, for which Dramix 65/60 3D steel fibers were used with a higher percentage. So it can be said that steel fiber percentage is the dominating factor in the strength of these specimens. Among the specimens with the same steel fiber ratio of 0.75% and without PVA, SA3, the one with double hook-end Dramix 65/60 5D steel fibers resulted in the highest capacity. Better anchorage provided by double hook-end increased the bending capacity of this specimen as well. SA1, the specimen with shorter Dramix 35/45 3D steel fibers had the lowest capacity. Therefore, it can be said that shorter fibers in this specimen adversely affected the strength.

Addition of PVA had a negative effect in all specimens. PVA addition reduced the maximum load and load levels sustained after cracking. This result can be attributed to the deterioration in the homogeneity of the concrete mix due to the fibers. When there are more fibers in the mix, concrete becomes more heterogeneous, reducing its performance. This is more visible for SA4, where addition of PVA reduced the maximum load dramatically by 47%. Addition of PVA fibers disturbed the homogeneity of the mix that already contained high amount of steel fibers. Similarly, in SA3, decrease in maximum load was 27% when PVA fibers were added, which was higher than the case for SA1 and SA2, for which the reduction was 10% and 14%, respectively. Collection of PVA fibers around double hook-ends could have had a negative effect on the performance of these fibers higher than others.

4.2. Four-point Bending Tests

The specimens with the dimensions of $1.25 \times 0.5 \times 0.05$ m were tested under four-point bending. Results are given in following sections.

4.2.1. SA1a And SA1a+PVA

Total load- midspan deflection responses of SA1a and SA1a+PVA are presented in Figure 58 and photos of specimens at the final stage of the testing are given in Figure 59 and 60.

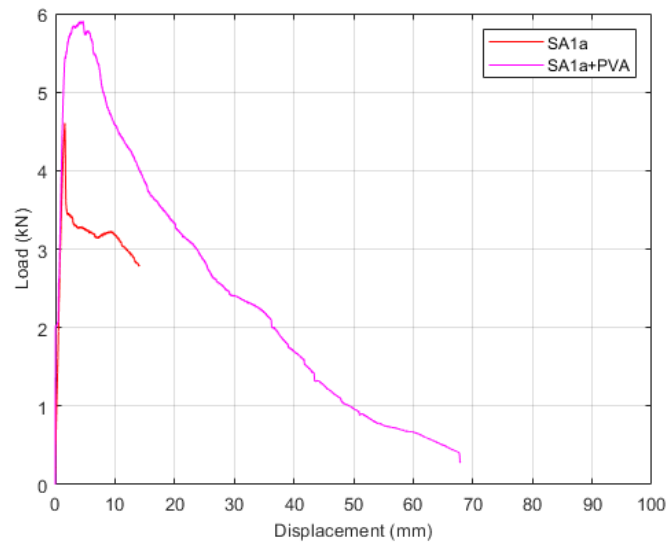


Figure 58: Load-midspan deflection response for SA1a and SA1a+PVA.

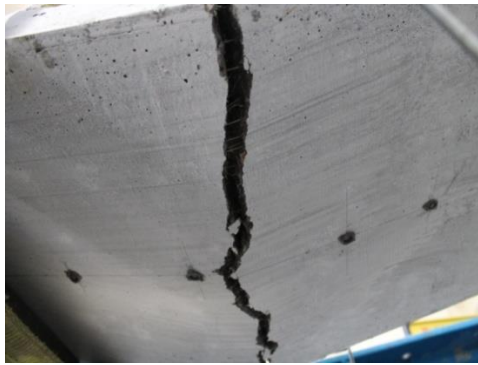


(a) Bottom view



(b) Side view

Figure 59: Final view of SA1a after testing.



(a) Bottom view



(b) Side view

Figure 60: Final view of SA1a + PVA after testing.

Dramix 35/45 3D steel fibers were used for these specimens. Specimen with only steel fibers, SA1a, sustained a total maximum load of 4.60kN, whereas SA1a+PVA sustained a higher level of load of 5.91kN, corresponding to 0.81kN.m and 1.03kN.m maximum moment capacities, respectively. As seen in figure, both specimens failed due to a single crack in the constant moment region at a point near to one of the applied loads. SA1a+PVA sustained higher levels of load after initial cracking whereas the load had a sudden drop after cracking in SA1a. Addition of PVA had a positive effect for these steel fibers.

4.2.2. SA2a And SA2a+PVA

Total load- midspan deflection responses of SA2a and SA2a+PVA are presented in Figure 61 and photos of specimens at the final stage of the testing are given in Figure 62 and 63.

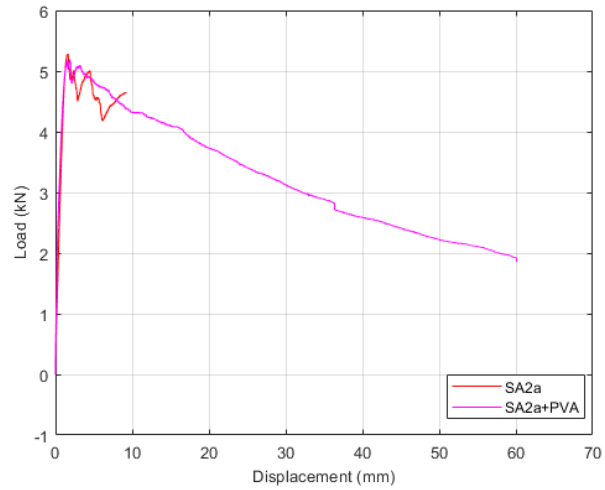
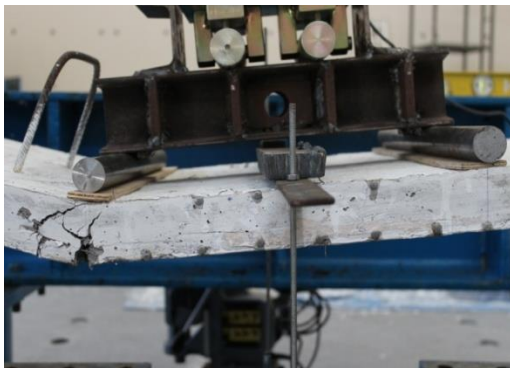


Figure 61: Load-midspan deflection response for SA2a and SA2a+PVA.



(a) Side view



(b) bottom view

Figure 62: Final view of SA2a after testing



(a) Near side view



(b) side view

Figure 63: Final view of SA2a+PVA after testing.

Single hook-end Dramix 65/60 3D steel fibers were used for these specimens. Specimen with only steel fibers, SA2a, sustained a maximum load of 5.29kN, whereas SA2a+PVA sustained a load of 5.19 kN, corresponding to 0.92kN.m and 0.91kN.m maximum moment capacities, respectively. As seen in figure, both specimens failed due to a single crack at one of the applied load points. Both specimens had a close load-deflection behavior.

4.2.3. SA3a And SA3a+PVA

Total load- midspan deflection responses of SA3a and SA3a+PVA are presented in Figure 64 and photos of specimens at the final stage of the testing are given in Figure 65 and 66.

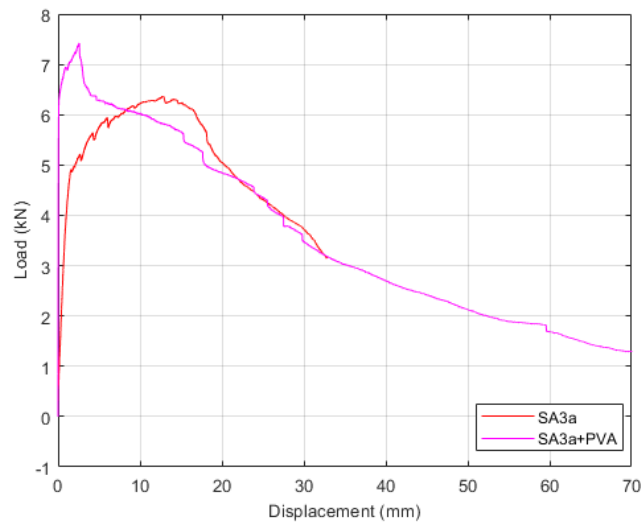


Figure 64: Load-midspan deflection response for SA3a and SA3a+PVA.

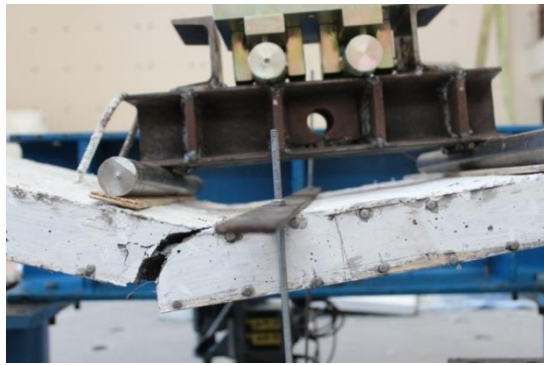


(a) Side view



(b) Bottom view

Figure 65 : Final view of SA3a after testing.



(a) Side view



(b) Bottom view

Figure 66: Final view of SA3a+PVA after testing

Double hook-end Dramix 65/605D steel fibers were used for these specimens. Specimen with only steel fibers, SA3a, sustained a maximum load of 6.37kN, whereas SA3+PVA sustained a higher level of load of 7.42 kN, corresponding to 1.11kN.m and 1.30kN.m maximum moment capacities, respectively. As seen in figure, both specimens failed due to a single crack close to a point of one of the applied loads. Although SA3a+PVA had a higher cracking load, its stiffness dropped steadily after cracking whereas SA3a had an increased load after cracking until about 15 mm midspan deflection after which the load started to drop. Load-deflection responses of both beams were very similar after about 20 mm deflection.

4.2.4. SA4a And SA4a+PVA

Total load- midspan deflection responses of SA4a and SA4a+PVA are presented in Figure 67 and photos of specimens at the final stage of the testing are given in Figure 68 and 69.

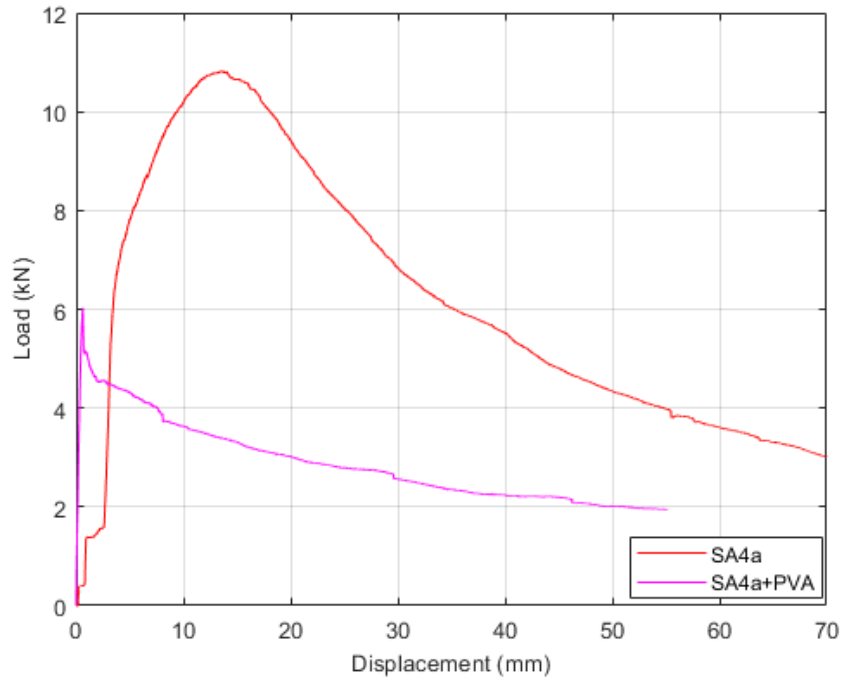
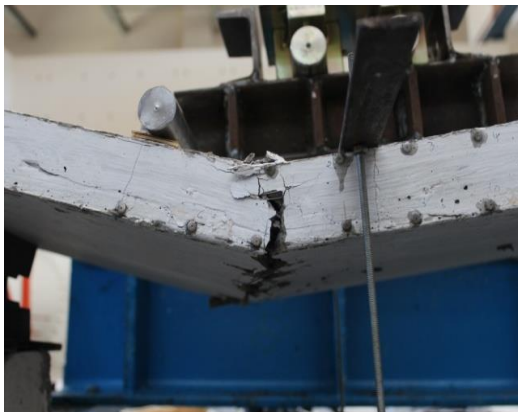


Figure 67: Load-midspan deflection response for SA4a and SA4a+PVA.



(a) Side view



(b) Bottom view

Figure 68: Final view of SA4a after testing.



(a) Side view

(b) Bottom view

Figure 69: Final view of SA4a+PVA after testing.

Single hook-end Dramix 65/603D steel fibers were used with a higher percentage for these specimens. Specimen with only steel fibers, SA4a, sustained a maximum load of 10.83 kN, whereas SA4a+PVA sustained a lower level of load of 6.03kN, corresponding to 1.90kN.m and 1.05kN.m maximum moment capacities, respectively. As seen in figure, both specimens failed due to a single crack at a point very near to the applied load. SA4a sustained considerably higher level of loads and reached higher level of displacements compared to SA4a+PVA. Addition of PVA had a serious adverse effect for this mix.

4.2.5. Discussion of Results For Four-point Bending Tests

Maximum load and moments obtained from four-point tests are summarized in Table 8 and Figure 70 and figure 71.

Table 8: Maximum total load and moments for four-point bending tests.

Specimen	Maximum Total Load (kN)	Maximum Moment (kN.m)
SA1a	4.60	0.81
SA1a+PVA	5.91	1.03
SA2a	5.29	0.92
SA2a+PVA	5.19	0.91
SA3a	6.37	1.11
SA3a+PVA	7.42	1.30
SA4a	10.83	1.90
SA4a+PVA	6.03	1.05

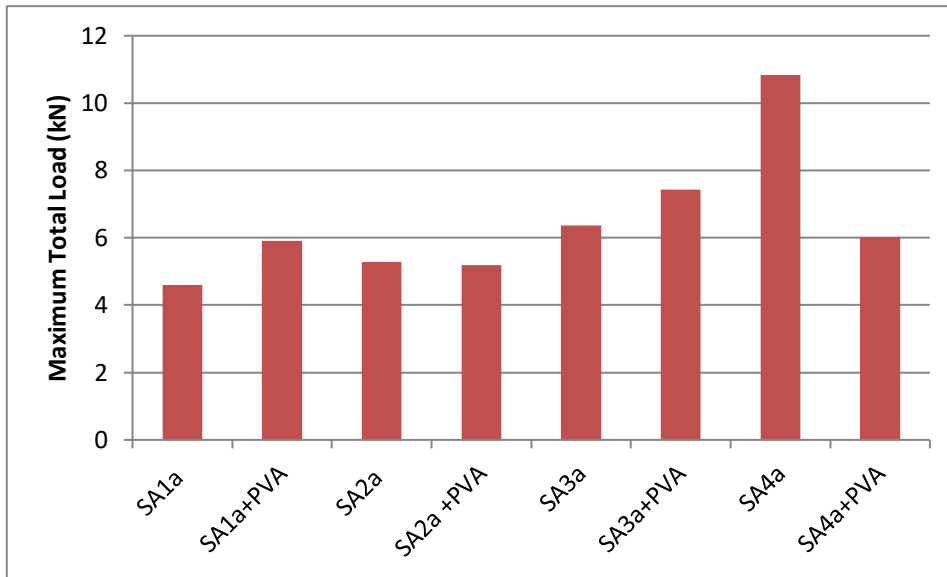


Figure 70: Maximum loads for four-point bending tests.

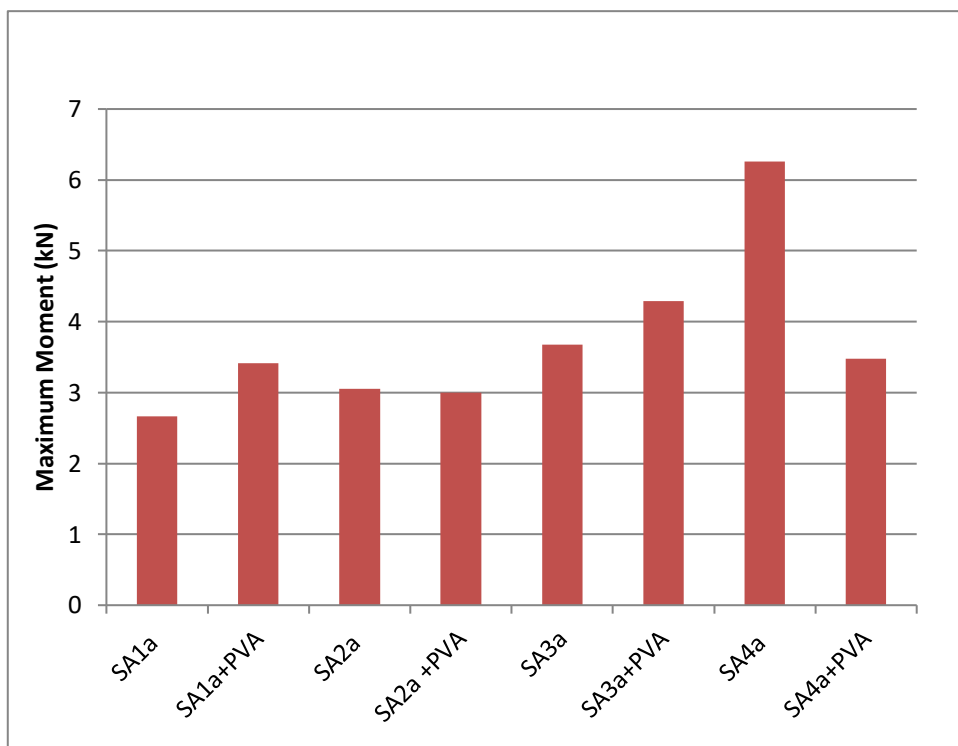


Figure 71: Maximum moments for four-point bending tests.

As it is seen from results, as far as specimens with only steel fibers concerned, general trend observed in load capacities for four-point tests were very similar to that of three-point tests. SA4, the specimen with the highest steel fiber ratio, reached the highest load whereas SA1, the specimen with shortest fibers, carried the least force.

When moment capacities obtained from specimens with only steel fibers are compared as in Figure 72, moment capacities obtained from three-point and four-point bending tests were very close for identical specimens, although the ones obtained from four-point bending were slightly higher than the three-point bending. However, in four-point bending tests, unlike the case for three-point bending, addition of PVA had a positive effect. Except for SA4a, addition of PVA increased the maximum load. Addition of PVA also improved the load-deflection behavior for SA1a, whereas the behavior with and without PVA was very similar for SA2a and SA3a. Addition of PVA for SA4a had an adverse effect, as was the case for three-point test. When moment capacities of specimens with PVA were compared for three- and four-point tests as done in Figure 73, it can be seen that for all specimens, moment capacities obtained from four-point tests were considerably higher than the ones obtained from three-point bending tests. In three-point bending tests, the maximum moment was at the midspan, which caused localization in cracking. Beams cracked by a single crack at the midspan for these specimens with no visible cracking at other locations. However, under four-point bending, maximum moment acts over a region at the middle, which caused several minor cracking along with the major crack. Under these conditions, addition of PVA fibers resulted in a better performance.

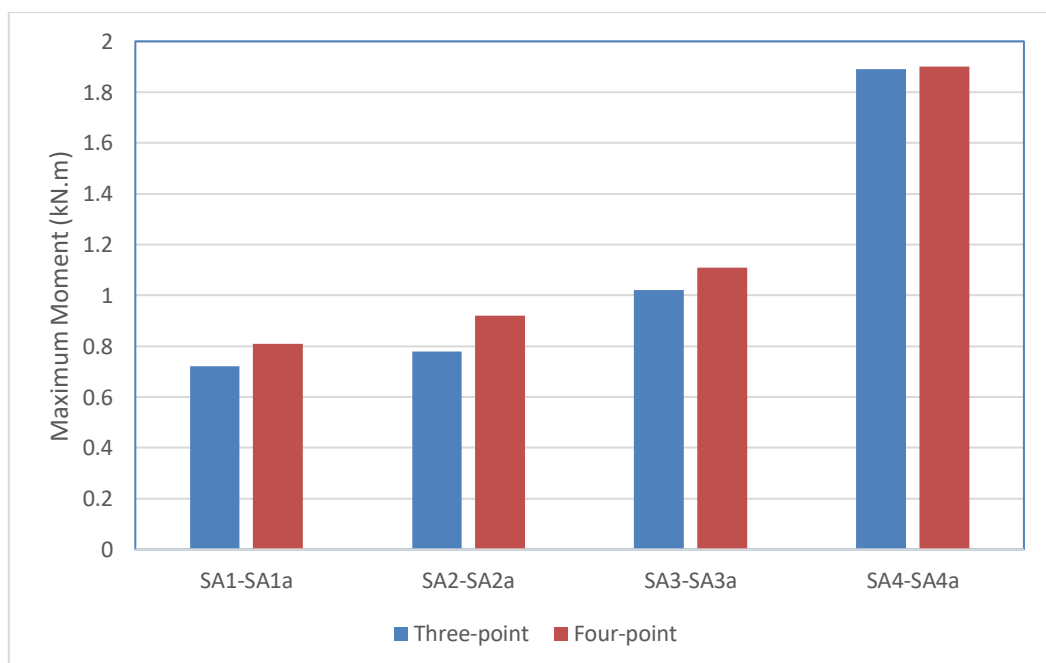


Figure 72: Maximum moments for steel fiber only specimens.

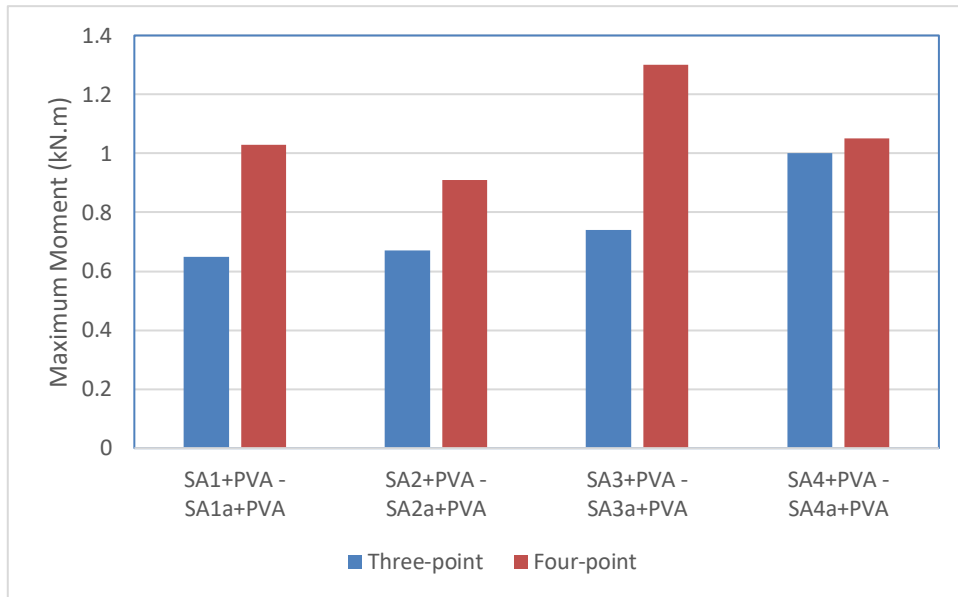


Figure 73: Maximum moments for specimens with PVA fibers.

4.3. The Compression Tests Results :

Results obtained from the compression test done on the cylinders with different mix designs are summarized from Table 9 to Table 12 and Figure 74.

Table 9: Cylinder compressive strengths for SA1 mix.

SA1 and SA1+PVA			
Mix	Specimen N ^o	Compression Strength(MPa)	Average (MPa)
Without any fiber	1	32.59	33.18
	2	35.47	
	3	31.49	
With steel fibers.	1	37.51	39.87
	2	45.53	
	3	36.57	
With steel and PVA fibers	1	39.57	39.87
	2	39.33	
	3	40.71	

Table 10: Cylinder compressive strengths for SA2 mix.

SA2 and SA2+PVA			
Mix	Specimen N°	Compression Strength (MPa)	Average (MPa)
Without any fiber	1	39.28	36.00
	2	36.6	
	3	32.13	
With steel fiber	1	37.68	38.52
	2	40.04	
	3	37.83	
With steel and PVA fibers	1	38.31	39.30
	2	41.3	
	3	38.3	

Table 11: Cylinder compressive strengths for SA3 mix.

SA3 and SA3+PVA			
Mix	Specimen N°	Compression Strength (MPa)	Average (MPa)
Without any fiber	1	27.5	30.93
	2	29.7	
	3	35.6	
With steel fiber	1	37.33	37.18
	2	38.18	
	3	36.4	
with steel and PVA fibers	1	44.07	38.27
	2	37.8	
	3	34.27	

Table 12: Cylinder compressive strengths for SA4 mix.

SA4 and SA4+PVA			
Mix	Specimen N°	Compression Strength (MPa)	Average (MPa)
Without any fiber	1	38	35.21
	2	30.84	
	3	36.79	
With steel fiber	1	33.39	35.53
	2	34.46	
	3	38.73	
with steel and PVA fibers	1	41.59	43.06
	2	42.46	
	3	45.12	

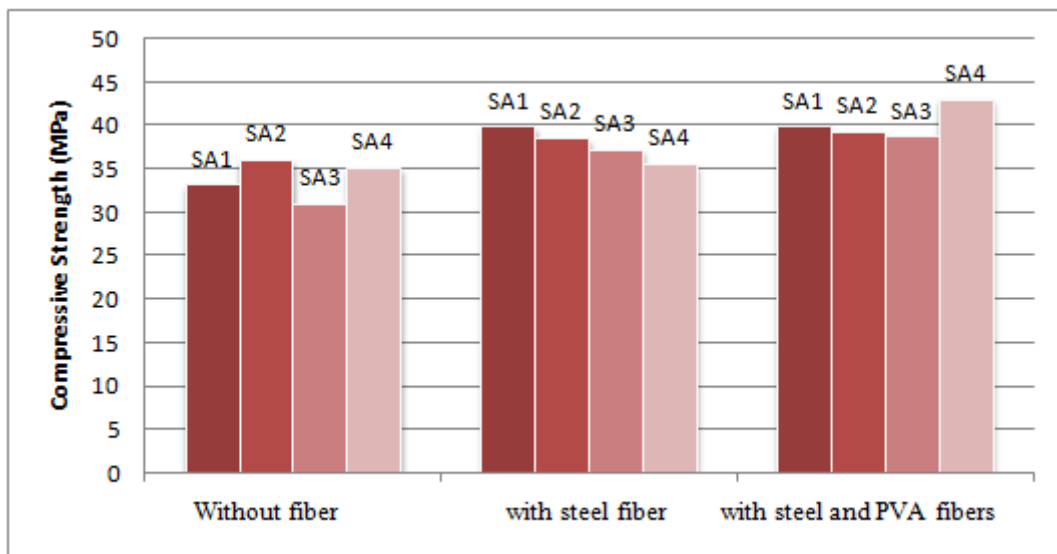


Figure 74: Compression strength for concrete mixes.

The compression testes done on the cylinders with different mix designs caused a slight improvement on the compressive strength of the specimens after adding the steel fiber and after adding the PVA fiber. The control specimen's compressive strength has the average of 33.83 MPa. For cylinders which contain steel fibers, compressive

strengths vary from 35.53 MPa to 39.87MPa for different mixes. For cylinders which contain both steel and PVA fibers, compressive strengths vary from 38.27 MPa to 43.06 MPa. It can be concluded that adding steel and PVA fibers increase the compressive strength. This increase can be slight in most cases. However, it should be noted that the main advantage of the fibers in concrete shows itself under tensile stresses rather than compressive stresses.

CHAPTER 5

CONCLUSION

In this study, contributions of steel and PVA fibers to the bending behavior of concrete beams were investigated. Three different types of steel fibers were used with two different steel fiber ratios. Effects of fiber hybridization through adding PVA fibers to these steel fibers reinforced concrete beams were studied through three- and four-point bending tests applied on beams. Total of nine specimens were cast, including one control specimen without fibers. Remaining eight specimens were cast in pair of same steel fiber content, one of which had addition PVA fibers forming a hybrid fiber reinforced concrete mix. Specimens were 2.5x0.5x0.05 m in size. After testing these specimens under three-point bending, half of the beams were also subjected to four-point bending tests.

In general steel fibers dominate the bending behavior. Specimens with shorter steel fibers sustained lowest level of loads whereas longer steel fibers consistently sustained higher level of loads. Steel fiber ratio was also dominant. Specimen with higher steel fiber ratio, 1.25% compared to 0.75% in others, sustained highest level of loads.

Hybrid fiber reinforced concrete specimens, which were obtained by adding PVA fibers with 0.25% ratio to their only-steel-fiber counterparts, yielded different results depending on the type of loadings. For three-point bending case, for which a single crack developed at the loading point with almost no damage in other areas, addition of PVA had a clear adverse effect on the behavior. These specimens sustained lower levels of peak and post-peak loads. Difference in peak loads was higher in specimens with double hook-end steel fibers and with higher steel fiber ratio. This suggests that addition of PVA disturbed the homogeneity of these mixes and resulted in a weakness. On the other hand, addition of PVA had a neutral or positive effect for the same beams under four-point bending, with the exception of the specimen with higher steel fiber ratio. In these specimens, due to distributed stresses at the constant moment region, there have been more cracking in addition to the main crack. Therefore, adverse effect observed under three-point bending was overcome for four-point bending.

Positive effect of PVA fibers was very significant for the shorter steel fibers. On the other hand, for the specimen with higher steel fiber ratio, PVA fibers had an adverse effect under four-point bending, similar to the case for three-point bending.

Although there are numerous studies in the literature about the advantages of hybrid fiber reinforced concrete, as this study revealed, these benefits are not unconditional. Fiber addition disturbs the homogeneity of the concrete mix, which may have an adverse effect. Also it has to be noted that PVA fibers are typically used for higher strength concrete, for which they are more effective due to better bonding. In this study, normal strength concrete was used to reflect a more general concrete type. For these reasons, caution should be observed when fiber hybridization is preferred to increase the ductility of concrete under bending.

REFERENCES

- Abadel, Aref. 2016. "Mechanical Properties of Hybrid Fibre-Reinforced Concrete – Analytical Modelling and Experimental Behaviour" 68 (16).
- ACI 544. 1999. "ACI 544.4R-88: Design Considerations for Steel Fiber Reinforced Concrete." *ACI Committee 544 88* (Reapproved): 18.
- Alberti, M G, A Enfedaque, and J C Gálvez. 2017. "Fibre Reinforced Concrete with a Combination of Polyolefin and Steel-Hooked Fibres" 171: 317–25. <https://doi.org/10.1016/j.compstruct.2017.03.033>.
- Caggiano, Antonio, Serena Gambarelli, Enzo Martinelli, Nicola Nisticò, and Marco Pepe. 2016. "Experimental Characterization of the Post-Cracking Response in Hybrid Steel / Polypropylene Fiber-Reinforced Concrete" 125: 1035–43. <https://doi.org/10.1016/j.conbuildmat.2016.08.068>.
- Chasioti, Stamatina G, and Frank J Vecchio. 2017. "Effect of Fiber Hybridization on Basic Mechanical Properties of Concrete," no. 114. <https://doi.org/10.14359/51689479>.
- Hameed, Rashid, Alain Sellier, Anaclet Turatsinze, and Frédéric Duprat. 2013. "Flexural Behaviour of Reinforced Fibrous Concrete Beams : Experiments and Analytical Modelling." *Pak J. of Engineering and Applied Science* 13: 19–28.
- Kaur, Parveen, and Mohit Talwar. 2017. "Different Types of Fibres Used in FRC." *International Journal of Advanced Research in Computer Science* 8 (4): 2015–18. <https://www.ijarcs.info/index.php/Ijarcs/article/viewFile/3782/3263>.
- Maalej, M, Toshiyuki Hashida, and Victor Li. 2011. "Flexural Strength of Fiber Cementitious Composites," no. March 2017.
- Paper, Conference, Mohammad Musa Alami, Tahir Kemal Erdem, and Serdar Aydin. 2018. "Development of a Proper Mix-Design for Impact Loading of Deflection Hardening Hybrid Fiber Reinforced Concrete," no. 112. <https://doi.org/10.1007/978-94-024-1194-2>.

Singh, Harvinder. 2015. "Flexural Modeling of Steel Fiber-Reinforced Concrete Members: Analytical Investigations" 20 (4): 1–10. [https://doi.org/10.1061/\(ASCE\)SC.1943-5576.0000244](https://doi.org/10.1061/(ASCE)SC.1943-5576.0000244).

Zhang, Peng, Yifeng Ling, Juan Wang, and Yan Shi. 2019. "Bending Resistance of PVA Fiber Reinforced Cementitious Composites Containing Nano-SiO₂." *Nanotechnology Reviews* 8 (1): 690–98. <https://doi.org/10.1515/ntrev-2019-0060>.

<https://www.bekaert.com/en/products/construction/concrete-reinforcement/dramix-steel-fiber-concrete-reinforcement-solutions> Retrieved February 15, 2021